

Original Article

Pterostilbene exerts anti-cancer activity via endoplasmic reticulum stress activation in human lung adenocarcinoma cells

Guangfeng Su¹, Wenjian Liu², Hao Chen³, Xinhua Sun⁴

¹Department of Thoracic Surgery, The Affiliated Hospital of Shandong University of Traditional Chinese Medicine, Jinan, Shandong, China; ²Department of Oncology, The Affiliated Hospital of Taishan Medical University, Tai'an, Shandong, China; ³Department of Pharmacy, Qilu Hospital of Shandong University, Jinan, Shandong, China; ⁴Department of Surgery, Boshan District Hospital of Traditional Chinese Medicine, Zibo, Shandong, China

Received March 5, 2016; Accepted June 5, 2016; Epub August 15, 2016; Published August 30, 2016

Abstract: Pterostilbene (Pte), an analog of resveratrol, exerts a potent anti-cancer effect. In this study, we investigated the anticancer activity of Pte against human lung adenocarcinoma cells in vitro and explored the role of endoplasmic reticulum stress (ERS) in this process. Pte treatment resulted in a dose-dependent decrease in the viability of human lung adenocarcinoma A549 cells. Additionally, Pte exhibited potent anticancer activity, as evidenced by reduction in intracellular glutathione (GSH) level and increases in the apoptotic index, caspase-3 activity, and reactive oxygen species. Furthermore, Pte treatment increased the expression of ERS-related molecules (p-PERK, ATF6, GRP78, and CHOP). These data indicate that Pte is a potential inhibitor of lung adenocarcinoma cell growth by targeting ERS signaling and suggest that the activation of ERS signaling may represent a novel therapeutic intervention for lung adenocarcinoma.

Keywords: Pterostilbene, lung adenocarcinoma, endoplasmic reticulum stress

Introduction

Lung cancer is the leading cause of cancer-related death worldwide, with annual deaths due to this disease increasing rapidly [1]. Non-small cell lung cancer (NSCLC) subtypes (adenocarcinoma, squamous cell carcinoma and large cell carcinoma) account for 80-85% of all lung cancers. Most patients with NSCLC are diagnosed with advanced stages and have inoperable local or distant metastases [2]. Although there have been significant advances in the treatment of lung adenocarcinoma due to the introduction of novel chemotherapies combined with targeted agents, the overall survival rate remains low. Therefore, there is a great need for novel therapeutic agents, specifically chemopreventive agents derived from less harmful natural materials.

Pterostilbene (3,5-dimethoxy-4'-hydroxystilbene, Pte), a natural dimethylated analog of resveratrol from blueberries, is known to exhibit diverse pharmacological activities, including

anticancer, anti-inflammation, antioxidant, anti-proliferative and analgesic properties [3]. Pte has potent antitumor activities with low toxicity in various cancer types, including breast cancer [4], liver cancer [5], and prostate cancer [6]. Studies have also shown that resveratrol can induce the apoptosis of lung cancer cells [7, 8]. However, the effects of Pte on human adenocarcinoma and the mechanisms responsible for these effects have not been elucidated.

The endoplasmic reticulum (ER) is a type of organelle in the cells of eukaryotic organisms whose membranes are continuous with the outer membrane of the nuclear envelope. There are numerous factors leading to functional and structural disorders of the ER, referred to as ER stress (ERS), including malnutrition, hypoxia and disturbance of calcium homeostasis and protein glycosylation. ERS often results in unfolded or misfolded proteins accumulating in the ER, consequently activating the unfolded protein response (UPR) [9]. Thus, the characteristic molecules of the three UPR pathways are

Pterostilbene exerts anti-cancer activity via ERS activation

used to describe the development of ERS, including PKR-like ER kinase (PERK), inositol-requiring enzyme 1 (IRE1), and activating transcription factor 6 (ATF6), which are collectively referred to as ERS sensors [10]. Under normal conditions, these three molecules remain inactive due to interactions with the immunoglobulin heavy chain binding protein, also known as glucose-regulated protein 78 (GRP78). However, when there is an increase in unfolded proteins in the ER lumen, GRP78 is disaggregated from UPR-related proteins and then binds to unfolded proteins to promote protein folding. The release of GRP78 from PERK, IRE1 and ATF6 leads to their activation as well as to downstream signaling involving the α -subunit of eukaryotic translational initiation factor 2 α (eIF2 α), C/EBP homologous protein (CHOP), and apoptotic family members [11, 12]. And ERS activation can induce cell death in human breast carcinoma cell lines [11]. However, the role of ERS signaling in the anti-NSCLC activity of Pte has not been investigated. In the present study, we assessed the anti-cancer activity of Pte in human lung adenocarcinoma cells and explored the role of ERS signaling in this process.

Materials and methods

Reagents

Pte, dimethyl sulfoxide (DMSO), and 2',7'-dichlorofluorescein diacetate (DCFH-DA) were purchased from the Sigma-Aldrich Company (St. Louis, MO, USA). Terminal deoxynucleotidyl transferase/UTP nick-end labeling (TUNEL) kits were purchased from Roche (Mannheim, Germany). The cell counting kit-8 was purchased from Dojindo (Kumamoto, Japan). The caspase-3 cellular activity assay kit was purchased from Merck (MBL International Corporation, Woburn, MA, USA). Glutathione (GSH) kit was obtained from the Nanjing Jiancheng Bio-engineering Institute (Nanjing, Jiangsu, China). Antibodies against GRP78, ATF6, phosphorylated-PERK (p-PERK), PERK, and CHOP were obtained from Santa Cruz Biotechnology (Santa Cruz, CA, USA). The antibody against β -actin was obtained from Cell Signaling Technology (Beverly, MA, USA).

Cell culture and treatment

Human A549 lung adenocarcinoma cells were obtained from the Cell Culture Center, Chinese

Academy of Medical Sciences (Shanghai, China). The cells were cultured in Dulbecco's modified Eagle's medium (Gibco, Grand Island, NY, USA) supplemented with 10% fetal bovine serum (Gibco), L-glutamine (2 mM), penicillin (100 units/ml), streptomycin (100 units/ml) and HEPES (25 mM). The cells were maintained in the presence of 5% CO₂ at 37°C. A PTE stock solution was prepared in DMSO and diluted with culture medium immediately prior to the experiment. DMSO (0.01%) was used as the control. The cells were treated with PTE (1.5, 3 or 6 mM), and a proper concentration was chosen in the following experiments.

Assay of cell viability

The cell count kit-8 assay was employed to quantitatively evaluate cell viability. The cultured A549 cells were carefully washed twice with PBS and then removed using 0.25% trypsin. The cells were collected by centrifugation at 1200 rpm for 3 min. Next, the A549 cells were plated in 96-well plates at a density of 6000 cells per well in 100 μ L of DMEM medium supplemented with 10% FBS; six parallel replicates were prepared, followed by exposure to various treatments. The control group was treated with 0.1% DMSO. Next, 10 μ L of CCK-8 was added to each well and the plates were incubated at 37°C in a 5% CO₂/95% air humidified incubator for 2 h. Then, optical density (OD) values were assessed at 450 nm using a microplate reader (SpectraMax 190, Molecular Devices, USA), and the cell viability was expressed as the OD value [13]. The cell morphology was obtained under an inverted/phase contrast microscope and images were taken using a 600D camera (Canon Company, Japan). All experiments were repeated three times.

Analysis of cell apoptosis

Apoptosis was measured using TUNEL staining. Briefly, after the different treatments, the A549 cells grown on cover slips were washed twice with PBS, fixed in 4% paraformaldehyde for 30 min, followed by blockade of endogenous peroxidase activity with 3% hydrogen peroxide diluted in methanol for 10 min at room temperature. Cells were then incubated in 0.1% Triton X-100 for 5 min on ice. After washing with PBS, cells were covered with 75 μ L of TUNEL reaction mixture. Next, all of the cell samples were

Pterostilbene exerts anti-cancer activity via ERS activation

incubated in this solution for 60 min at 37°C in a humidified dark chamber. Finally, cells were stained with DAPI before they were visualized under an Olympus FV1000 (Olympus, Japan) confocal microscope. All of the digital images were taken using an image analyzing system (Image Pro Plus, Media Cybernetics, Rockville, MD, USA). Then, the mean optical density (MOD) of the positive staining cells and the positive expression area ratio (positive nuclei occupying a total area in the visible field compared with the total percentage of all nuclei in the field) were assessed in 10 randomly selected fields. Finally, the apoptosis index (AI) was calculated using the following formula: $AI (\%) = MOD \times \text{expression area ratio} \times 100$. The AI value in the control group was set to 100%.

Analysis of caspase-3 activity

According to the manufacturer's recommendations, caspase-3 activity was measured using a colorimetric assay kit. The cells were washed in ice-cold PBS, and the proteins were extracted then stored at -80°C. The cell protein liquid samples (20 µL) were added to a buffer that contained a p-nitroaniline(pNA)-conjugated substrate for caspase-3 (Ac-DEVD-pNA) to yield a 100-µL total reaction volume. Incubations were placed at 37°C. The released pNA concentrations were calculated based on the absorbance values at 405 nm and the calibration curve of the defined pNA solutions. The caspase-3 activity in the control group was set as 100%.

Analysis of intracellular ROS generation

DCFH-DA passes through cell membranes and is cleaved by esterases to yield DCFH. ROS oxidize DCFH, generating the fluorescent compound dichlorofluorescein, which can be used for quantification. After being treated with Pte (1.5, 3 or 6 mM) for 24 h, the cells were trypsinized and subsequently incubated with DCFH-DA (20 mM) in PBS at 37°C for 2 h. After incubation, the DCFH fluorescence of the cells in each well was measured using an FLX 800 microplate fluorescence reader with 530 nm as the emission wavelength and 485 nm as the excitation wavelength (Biotech Instruments Inc., USA). The background was determined using cell-free conditions. The fluorescence intensity in the control group was defined as 100%.

Analysis of the intracellular GSH level

The GSH level was determined in cells using a glutathione kit as described previously [14]. Briefly, cells were plated at a density of 1×10^6 in 100 mm culture dishes and allowed to attach overnight. The cells were treated on the second day with Pte. The cells were collected by scraping and washed with PBS, and the cell lysate was used to determine the GSH level (using the above-mentioned kit) according to the manufacturer's instructions. The GSH level in the control group was set to 100%.

Western blot

The cells were scraped off and then lysed in sample buffer [150 mM Tris (pH 6.8), 8 M urea, 50 mM DTT, 2% sodium dodecyl sulfate, 15% sucrose, 2 mM EDTA, 0.01% bromophenol blue, 1% protease, and phosphatase inhibitor cocktail], sonicated, boiled, run through an SDS-PAGE gel and transferred to an Immobilon NC membrane (Millipore, Billerica, MA, USA). The membranes were blocked with 5% BSA in TBST [150 mM NaCl, 50 mM Tris (pH 7.5), 0.1% Tween-20] and then probed with antibodies against p-PERK, PERK, ATF6, GRP78, and CHOP (1:500) and against β -actin (1:1000) overnight at 4°C. Next, the membranes were washed with TBST, probed with secondary antibodies (1:5000) in blocking buffer at room temperature for 2 h and washed. The fluorescence was detected using a BioRad imaging system (BioRad, West Berkeley, California, USA), and the signals were quantified using the Image Lab Software (BioRad, West Berkeley, California, USA).

Statistical analysis

All of the values are presented as the mean \pm standard deviation (S.D.). Group comparisons were performed using ANOVA (SPSS 13.0). All of the groups were analyzed simultaneously using the LSD-t test. $P < 0.05$ was considered to be statistically significant.

Results

Effects of Pte treatment on the viability of human lung adenocarcinoma cells

The CCK-8 assay was used to evaluate the effect of Pte on A549 cells. The treatment of A549 cells for 24 h with 1.5, 3 or 6 mM of Pte

Pterostilbene exerts anti-cancer activity via ERS activation

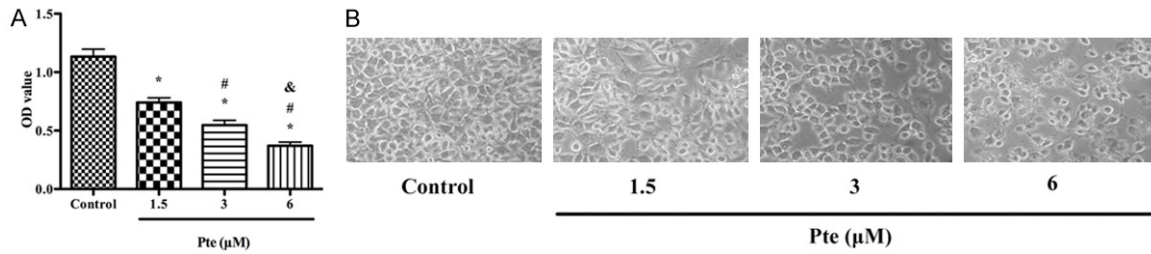


Figure 1. Effect of Pte treatment on the viability of human lung adenocarcinoma cells. A. Cells were treated with different concentrations of Pte (1.5, 3, and 6 μM) and assessed at 24 h after treatment. Viability is expressed as OD value. B. Cell morphology was observed under an inverted phase contrast microscope after the cells were treated for 24 h, and images were obtained. Significant cell shrinkage and a decreased cellular attachment rate were observed in the Pte treatment groups. All of the data are expressed as the mean ± SD, n = 6 for each group. * $P < 0.05$ versus the control group, # $P < 0.05$ versus the 1.5 μM Pte-treated group, & $P < 0.05$ versus the 3 μM Pte-treated group.

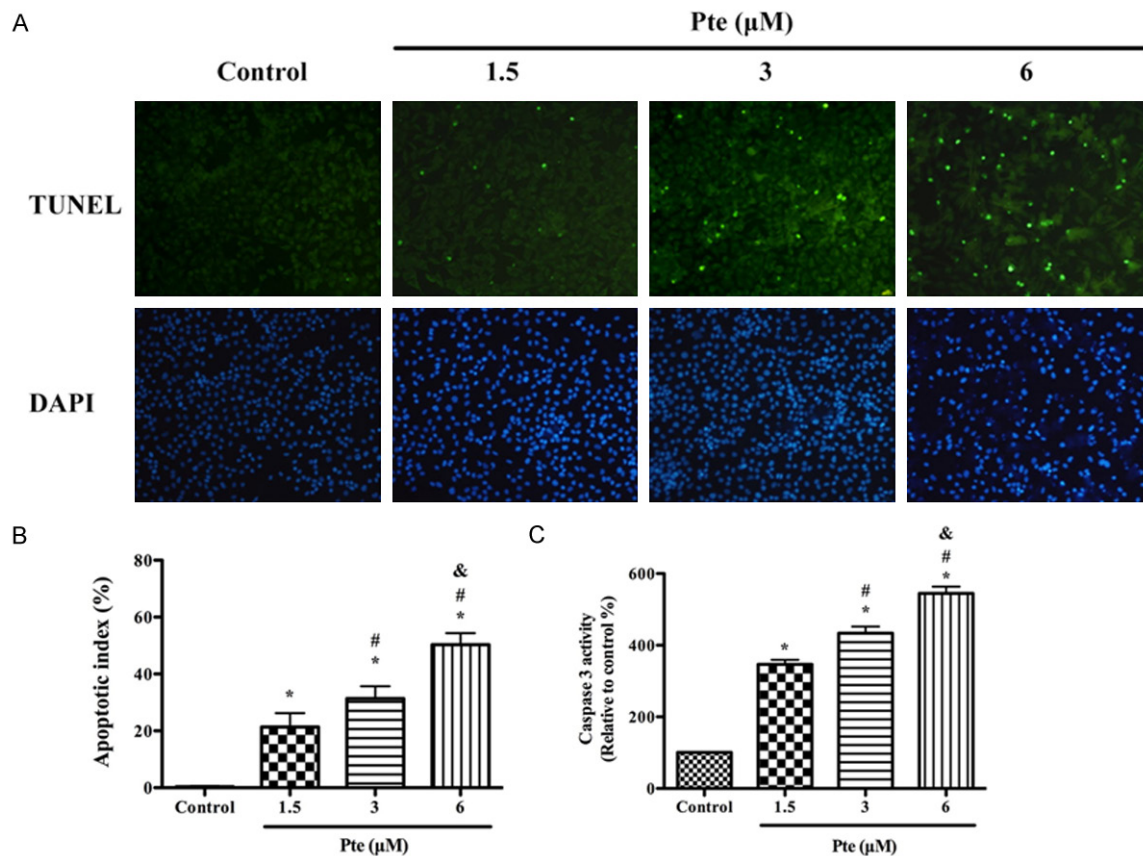


Figure 2. Effect of Pte treatment on the apoptosis of human lung adenocarcinoma cells. A and B. The apoptotic index of Pte-treated lung adenocarcinoma cells showed a dose-dependent increase. C. Pte treatment induced the increase of caspase-3 activity in a dose-dependent manner. All of the data are expressed as the mean ± SD, n = 6 for each group. * $P < 0.05$ versus the control group, # $P < 0.05$ versus the 1.5 μM Pte-treated group, & $P < 0.05$ versus the 3 μM Pte-treated group.

resulted in cell growth inhibition in a dose-dependent manner (Figure 1A). The microscopy images showed that Pte treatment resulted in significant cell shrinkage and a decrease in the rate of cellular attachment compared with the control treatment (Figure 1B).

Effects of Pte treatment on the apoptosis of human lung adenocarcinoma cells

After treatment with 1.5, 3 or 6 mM of Pte for 24 h, the apoptotic index was increased in a dose-dependent manner (Figure 2A, 2B). Pte

Pterostilbene exerts anti-cancer activity via ERS activation

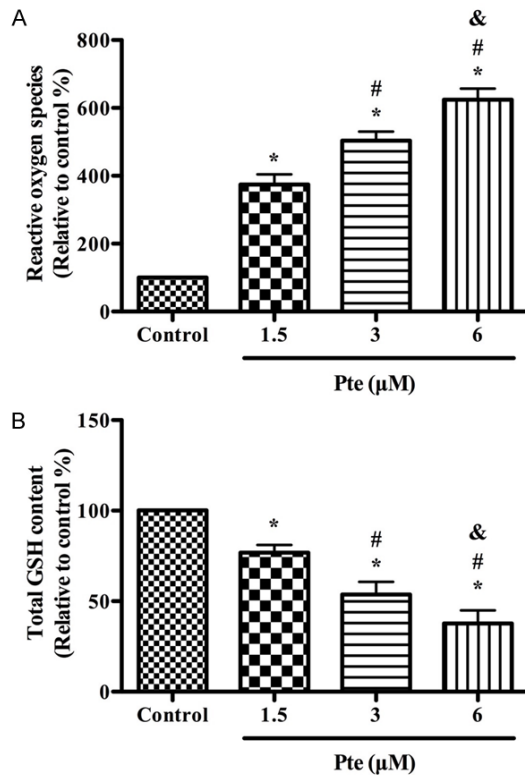


Figure 3. Effect of Pte treatment on ROS generation, and the GSH level of human lung adenocarcinoma cells (24 h). A. ROS productions are shown. The fluorescence intensity in the control group was defined as 100%. B. Intracellular GSH levels are shown. The GSH levels in the control group were defined as 100%. All of the data are expressed as the mean \pm SD, $n = 6$ for each group. * $P < 0.05$ versus the control group, # $P < 0.05$ versus the 1.5 μM Pte-treated group, & $P < 0.05$ versus the 3 μM Pte-treated group.

treatment also increased caspase-3 activity in a dose-dependent manner (Figure 2C). These results provide convincing data that Pte can induce apoptosis of A549 cells.

Effects of Pte treatment on ROS generation, and the GSH level of human lung adenocarcinoma cells

To measure the effect of Pte on intracellular oxidation, the specific oxidation-sensitive fluorescent dye DCFH-DA was used. The fluorescent intensity of this dye is increased following the generation of intracellular reactive metabolites. The treatment of A549 cells with Pte (1.5, 3 or 6 μM) for 24 h induced a dose-dependent increase in ROS generation (Figure 3A).

Reduced GSH is the major non-protein thiol in cells and is essential for maintaining the cellu-

lar redox status [15]. The treatment of A549 cells with Pte (1.5, 3 or 6 μM) for 24 h induced a dose-dependent decrease in the intracellular GSH level (Figure 3B). These results suggest that Pte treatment affects the cellular redox status of the A549 cells.

Effects of Pte on ERS signaling in human lung adenocarcinoma cells

To investigate the role of ERS signaling in Pte anticancer effect, ERS-related molecules were detected by Western blot. As shown in Figure 4, Pte treatment induced a dose-dependent up-regulation of the p-PERK, ATF6, GRP78, and CHOP protein levels in A549 cells.

Discussion

As a natural dimethylated analog of resveratrol, Pte has been shown to suppress the proliferation of various types of cancer cells, including pancreatic, breast, colon, oral, lung, prostate carcinoma cells, melanoma, myeloma, and leukemia cells [4-6]. Various molecules and signaling pathways are involved in the anti-tumor effects of Pte, including cytosolic Ca^{2+} overload [4], adenosine monophosphate activated protein kinase (AMPK) signaling [6], autophagy [16], ROS [16], and lysosomal membrane permeabilization [17]. However, the effects of Pte of human lung adenocarcinoma and the mechanisms responsible for these effects are not fully understood. In the present study, Pte treatment resulted in a dose-dependent inhibition of the viability of lung adenocarcinoma cells via ERS activation.

GSH is the main non-protein antioxidant in the cell. GSH can inactivate superoxide anion free radicals and provide electrons for enzymes such as glutathione peroxidase, which reduces H_2O_2 to H_2O . Reduced GSH is the major non-protein thiol in cells and is essential for maintaining the cellular redox status. The intracellular GSH content has a decisive effect on anti-cancer drug-induced apoptosis, and the apoptotic effects are inversely proportional to the GSH content [15]. In addition, ROS production is associated with the apoptotic response induced by anticancer agents [18]. Our results show that Pte can significantly increase ROS production and decrease GSH content in lung adenocarcinoma cells.

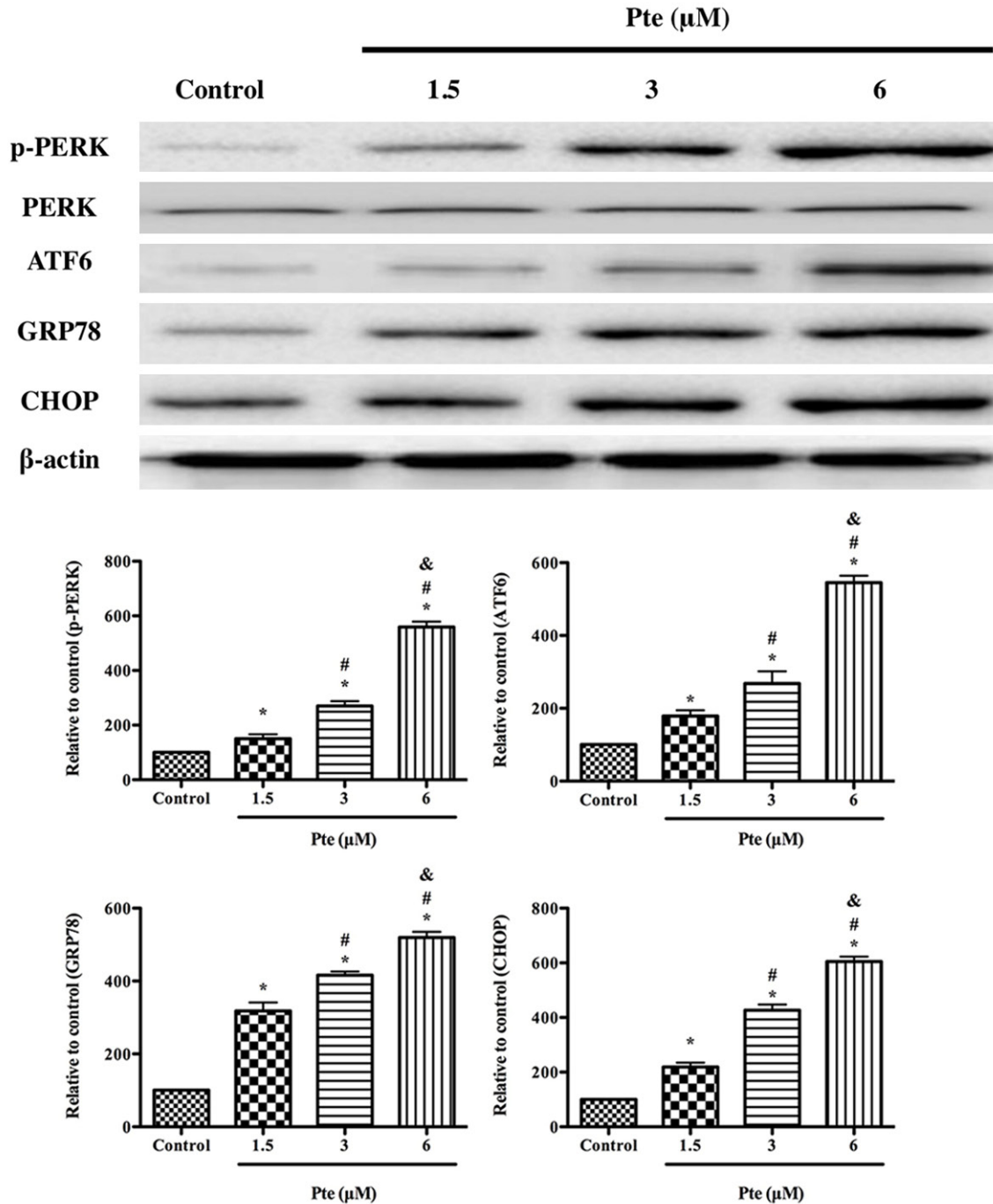


Figure 4. Effect of Pte on ERS signaling in human lung adenocarcinoma cells (24 h). Representative Western blot results of p-PERK, ATF6, GRP78, and CHOP are shown. All of the data are expressed as the mean \pm SD, $n = 6$ for each group. * $P < 0.05$ versus the control group, # $P < 0.05$ versus the 1.5 μM Pte-treated group, & $P < 0.05$ versus the 3 μM Pte-treated group.

ROS has been identified as a potential target for novel anticancer drugs. Studies have suggested that ERS could be either a cause or a result of increased ROS generation [19]. For instance, the activation of the PERK pathway

triggers the activation of transcription factor 4 (ATF4) and CHOP transcription factors. CHOP alone or in combination with ATF4 controls the expression of ER oxidoreductin-1 (Ero1) [20], which stimulates both mitochondrial and Nox2-

dependent ROS production [21]. GSH in the ER not only controls the activation state of Ero1 but also supports the reductive proofreading of aberrant disulfide bridges by PDIs [22]. In our study, the suppressive effect of Pte on A549 cells was associated with excessive activation of ERS and over-production of intracellular ROS.

The fate of cells subjected to ERS depends on the balance between cell adaptive and cell death responses. ERS generally plays a protective role in tumor development by activating adaptive stress response elements and attenuating apoptotic pathways. However, forced activation of ERS can lead to the reactivation of ERS-induced apoptosis, which can inhibit tumor development, growth and invasion [23]. In the present study, we explored the role of ERS in the anticancer effect of Pte against human lung adenocarcinoma cells. Our results indicated that Pte treatment up-regulated p-PERK, ATF6, GRP78, and CHOP expression in A549 cells, suggesting that the anticancer activity of Pte in lung adenocarcinoma cells is strongly associated with the activation of ERS signaling.

In summary, our study provides evidence that Pte is a potent inhibitor of human lung adenocarcinoma cell growth by activating ERS signaling. The activation of ERS signaling may represent a novel strategy to prevent the induction of cancer survival mechanisms in human lung adenocarcinomas. Pte may be developed as a therapeutic agent against advanced lung adenocarcinoma in the clinical settings.

Disclosure of conflict of interest

None.

Address correspondence to: Guangfeng Su, Department of Thoracic Surgery, The Affiliated Hospital of Shandong University of Traditional Chinese Medicine, No. 16369 Jingshi Road, Jinan 250014, Shandong, China. E-mail: thoracic0123@sina.com

References

- [1] Jemal A, Bray F, Center MM, Ferlay J, Ward E and Forman D. Global cancer statistics. *CA Cancer J Clin* 2011; 61: 69-90.
- [2] Cao M, Hou D, Liang H, Gong F, Wang Y, Yan X, Jiang X, Wang C, Zhang J, Zen K, Zhang CY and Chen X. miR-150 promotes the proliferation and migration of lung cancer cells by targeting

- SRC kinase signalling inhibitor 1. *Eur J Cancer* 2014; 50: 1013-1024.
- [3] McCormack D and McFadden D. Pterostilbene and cancer: current review. *J Surg Res* 2012; 173: e53-61.
- [4] Moon D, McCormack D, McDonald D and McFadden D. Pterostilbene induces mitochondrially derived apoptosis in breast cancer cells in vitro. *J Surg Res* 2013; 180: 208-215.
- [5] Pan MH, Chiou YS, Chen WJ, Wang JM, Badmaev V and Ho CT. Pterostilbene inhibited tumor invasion via suppressing multiple signal transduction pathways in human hepatocellular carcinoma cells. *Carcinogenesis* 2009; 30: 1234-1242.
- [6] Lin VC, Tsai YC, Lin JN, Fan LL, Pan MH, Ho CT, Wu JY and Way TD. Activation of AMPK by pterostilbene suppresses lipogenesis and cell-cycle progression in p53 positive and negative human prostate cancer cells. *J Agric Food Chem* 2012; 60: 6399-6407.
- [7] Ma L, Li W, Wang R, Nan Y, Wang Q, Liu W and Jin F. Resveratrol enhanced anticancer effects of cisplatin on non-small cell lung cancer cell lines by inducing mitochondrial dysfunction and cell apoptosis. *Int J Oncol* 2015; 47: 1460-1468.
- [8] Zhang L, Dai F, Sheng PL, Chen ZQ, Xu QP and Guo YQ. Resveratrol analogue 3,4,4'-trihydroxy-trans-stilbene induces apoptosis and autophagy in human non-small-cell lung cancer cells in vitro. *Acta Pharmacol Sin* 2015; 36: 1256-1265.
- [9] Wang G, Liu K, Li Y, Yi W, Yang Y, Zhao D, Fan C, Yang H, Geng T, Xing J, Zhang Y, Tan S and Yi D. Endoplasmic reticulum stress mediates the anti-inflammatory effect of ethyl pyruvate in endothelial cells. *PLoS One* 2014; 9: e113983.
- [10] Yin J, Gu L, Wang Y, Fan N, Ma Y and Peng Y. Rapamycin improves palmitate-induced ER stress/NF kappa B pathways associated with stimulating autophagy in adipocytes. *Mediators Inflamm* 2015; 2015: 272313.
- [11] Pan MY, Shen YC, Lu CH, Yang SY, Ho TF, Peng YT and Chang CC. Prodigiosin activates endoplasmic reticulum stress cell death pathway in human breast carcinoma cell lines. *Toxicol Appl Pharmacol* 2012; 265: 325-334.
- [12] Puthalakath H, O'Reilly LA, Gunn P, Lee L, Kelly PN, Huntington ND, Hughes PD, Michalak EM, McKimm-Breschkin J, Motoyama N, Gotoh T, Akira S, Bouillet P and Strasser A. ER stress triggers apoptosis by activating BH3-only protein Bim. *Cell* 2007; 129: 1337-1349.
- [13] Shi W, Nie D, Jin G, Chen W, Xia L, Wu X, Su X, Xu X, Ni L, Zhang X, Zhang X and Chen J. BDNF blended chitosan scaffolds for human umbilical cord MSC transplants in traumatic brain

Pterostilbene exerts anti-cancer activity via ERS activation

- injury therapy. *Biomaterials* 2012; 33: 3119-3126.
- [14] Huang PH, Chen JS, Tsai HY, Chen YH, Lin FY, Leu HB, Wu TC, Lin SJ and Chen JW. Globular adiponectin improves high glucose-suppressed endothelial progenitor cell function through endothelial nitric oxide synthase dependent mechanisms. *J Mol Cell Cardiol* 2011; 51: 109-119.
- [15] Zhao YF, Zhang C and Suo YR. MMPT as a reactive oxygen species generator induces apoptosis via the depletion of intracellular GSH contents in A549 cells. *Eur J Pharmacol* 2012; 688: 6-13.
- [16] Chakraborty A, Bodipati N, Demonacos MK, Peddinti R, Ghosh K and Roy P. Long term induction by pterostilbene results in autophagy and cellular differentiation in MCF-7 cells via ROS dependent pathway. *Mol Cell Endocrinol* 2012; 355: 25-40.
- [17] Mena S, Rodriguez ML, Ponsoda X, Estrela JM, Jaattela M and Ortega AL. Pterostilbene-induced tumor cytotoxicity: a lysosomal membrane permeabilization-dependent mechanism. *PLoS One* 2012; 7: e44524.
- [18] Liu Z, Li D, Zhao W, Zheng X, Wang J and Wang E. A potent lead induces apoptosis in pancreatic cancer cells. *PLoS One* 2012; 7: e37841.
- [19] Choi AY, Choi JH, Hwang KY, Jeong YJ, Choe W, Yoon KS, Ha J, Kim SS, Youn JH, Yeo EJ and Kang I. Licochalcone A induces apoptosis through endoplasmic reticulum stress via a phospholipase C γ 1-, Ca²⁺-, and reactive oxygen species-dependent pathway in HepG2 human hepatocellular carcinoma cells. *Apoptosis* 2014; 19: 682-697.
- [20] Marciniak SJ, Yun CY, Oyadomari S, Novoa I, Zhang Y, Jungreis R, Nagata K, Harding HP and Ron D. CHOP induces death by promoting protein synthesis and oxidation in the stressed endoplasmic reticulum. *Genes Dev* 2004; 18: 3066-3077.
- [21] Han J, Back SH, Hur J, Lin YH, Gildersleeve R, Shan J, Yuan CL, Krokowski D, Wang S, Hatzoglou M, Kilberg MS, Sartor MA and Kaufman RJ. ER-stress-induced transcriptional regulation increases protein synthesis leading to cell death. *Nat Cell Biol* 2013; 15: 481-490.
- [22] Kojer K and Riemer J. Balancing oxidative protein folding: the influences of reducing pathways on disulfide bond formation. *Biochim Biophys Acta* 2014; 1844: 1383-1390.
- [23] Chou TC and Talalay P. Quantitative analysis of dose-effect relationships: the combined effects of multiple drugs or enzyme inhibitors. *Adv Enzyme Regul* 1984; 22: 27-55.